

REPORT

Organics Captured from Comet 81P/Wild 2 by the Stardust Spacecraft

Scott A. Sandford,^{1*} Jérôme Aléon,^{2,3} Conel M. O'D. Alexander,⁴ Tohru Araki,⁵ Saša Bajt,⁶ Giuseppe A. Baratta,⁷ Janet Borg,⁸ John P. Bradley,⁶ Donald E. Brownlee,⁹ John R. Brucato,¹⁰ Mark J. Burchell,¹¹ Henner Busemann,⁴ Anna Butterworth,¹² Simon J. Clemett,¹³ George Cody,¹⁴ Luigi Colangeli,¹⁰ George Cooper,¹⁵ Louis D'Hendecourt,⁷ Zahia Djouadi,⁸ Jason P. Dworkin,¹⁶ Gianluca Ferrini,¹⁷ Holger Fleckenstein,¹⁸ George J. Flynn,¹⁹ Ian A. Franchi,²⁰ Marc Fries,¹⁴ Mary K. Gilles,²¹ Daniel P. Glavin,¹⁶ Matthieu Gounelle,²² Faustine Grossemy,⁸ Chris Jacobsen,¹⁸ Lindsay P. Keller,²³ A. L. David Kilcoyne,^{21,24} Jan Leitner,²⁵ Graciela Matrajt,⁹ Anders Meibom,²² Vito Mennella,¹⁰ Smail Mostefaoui,²² Larry R. Nittler,⁴ Maria E. Palumbo,⁷ Dimitri A. Papanastassiou,²⁶ François Robert,²² Alessandra Rotundi,²⁷ Christopher J. Snead,¹² Maegan K. Spencer,²⁸ Frank J. Stadermann,²⁹ Andrew Steele,¹⁴ Thomas Stephan,²⁵ Peter Tsou,²⁶ Tolek Tylliszczak,^{21,24} Andrew J. Westphal,¹² Sue Wirick,¹⁸ Brigitte Wopenka,³⁰ Hikaru Yabuta,¹⁴ Richard N. Zare,²⁸ Michael E. Zolensky³¹

Organics found in comet 81P/Wild 2 samples show a heterogeneous and unequilibrated distribution in abundance and composition. Some organics are similar, but not identical, to those in interplanetary dust particles and carbonaceous meteorites. A class of aromatic-poor organic material is also present. The organics are rich in oxygen and nitrogen compared with meteoritic organics. Aromatic compounds are present, but the samples tend to be relatively poorer in aromatics than are meteorites and interplanetary dust particles. The presence of deuterium and nitrogen-15 excesses suggest that some organics have an interstellar/protostellar heritage. Although the variable extent of modification of these materials by impact capture is not yet fully constrained, a diverse suite of organic compounds is present and identifiable within the returned samples.

Comets are small bodies that accreted in the outer solar system during its formation (1) and thus may consist of preserved samples of the “starting materials” from which the solar system was made. Organic materials are expected to be present in cometary samples (2) and may include molecules made and/or modified in stellar outflows, the interstellar medium, and the protosolar nebula, as well as by parent-body processing within the comet. The presence of organic compounds in comets and their ejecta is of astrobiological interest because their delivery to early Earth may have played an important role in the origin of life on Earth (3).

An overview of the Stardust mission and the collection and recovery of Wild 2 samples is provided elsewhere (4, 5). We describe the results obtained from the returned samples by the Stardust Organics Preliminary Examination Team (PET). Samples were studied using a wide range of analytical techniques, including two-step laser desorption laser ionization mass spectrometry (L²MS), liquid chromatography with UV fluorescence detection and time of flight mass spectrometry (LC-FD/TOF-MS), scanning transmission x-ray microscopy (STXM), x-ray absorption near-edge spectroscopy (XANES), infrared and Raman spectroscopy, ion chromatography with conductivity detection (IC), secondary ion mass spectrometry (SIMS), and time-of-flight SIMS (TOF-SIMS) (6). These techniques provide a wealth of information about the chemical nature and relative abundance of the organics in the samples. Our results are

compared with organic materials found in primitive meteorites and interplanetary dust particles (IDPs) collected in the stratosphere, as well as to astronomical and spacecraft observations of comets.

Despite some uncertainties associated with the presence of contaminants and alteration of the samples during the capture process, considerable information about the nature of the organics in the samples can be determined.

Some organic-containing contaminants are present in the returned sample collectors, but they are of low enough abundance or are sufficiently well characterized that they can be distinguished from the organics in the cometary materials in the returned samples (6). For example, the aerogel collector medium, which consists predominantly of amorphous SiO₂, contains from a quarter to a few weight percent C. However, nuclear magnetic resonance studies indicate that this C is largely in the form of simple Si-CH₃ groups easily distinguishable from the cometary organics described below. It should be noted that not all the collected organics in the samples will be fully representative of the original cometary material because some may have been modified during impact with the aerogel collectors. There is evidence that at least some organic compounds were generated or altered by impact heating of this material (6).

Multiple experimental techniques demonstrate that the samples contain polycyclic aromatic hydrocarbons (PAHs). L²MS spectra obtained from individual particles and in aerogel along impact tracks split lengthwise show PAHs and

their alkylated derivatives. Two distinct types of PAH distributions along tracks can be distinguished from the low backgrounds of PAHs present in the aerogel (figs. S1 and S2). In some cases, benzene and naphthalene (1- to 2-ring PAHs, including alkylation out to several CH₃ additions) are observed in the absence of moderate mass 3- to 6-ring PAHs (fig. S1). These distributions are uncharacteristic of meteorites and IDPs but resemble pyrolysis products of meteoritic macromolecular organics and are observed in high-power laser L²MS measurements of preflight and Stardust Witness aerogel tiles (6), raising the question about how many of the lower mass PAHs originate from impact processing of C original to the aerogel.

The second type of PAH population shows complex distributions that resemble those seen in

¹Astrophysics Branch, NASA-Ames Research Center, Moffett Field, CA 94035, USA. ²Glenn T. Seaborg Institute, Lawrence Livermore National Laboratory, Livermore, CA 94550 USA. ³Centre de Recherches Pétrographiques et Géochimiques, Vandoeuvre-les-Nancy, France. ⁴Department of Terrestrial Magnetism, Carnegie Institution, Washington, DC 20015–1305, USA. ⁵Department of Physics, North Carolina State University, Raleigh, NC 27695, USA. ⁶Institute of Geophysics and Planetary Physics, Lawrence Livermore National Laboratory, Livermore, CA 94550, USA. ⁷Istituto Nazionale di Astrofisica, Osservatorio Astrofisico di Catania, Via Santa Sofia 78, 95123 Catania, Italy. ⁸Institut d'Astrophysique Spatiale, Campus, 91405 Orsay Cedex, France. ⁹Department of Astronomy, University of Washington, Seattle, WA 98195, USA. ¹⁰INAF, Osservatorio Astronomico di Capodimonte, Via Moirariello 16, 80131 Napoli, Italy. ¹¹School of Physical Sciences, University of Kent, Canterbury, Kent CT2 7NH, UK. ¹²Space Sciences Laboratory, University of California at Berkeley, Berkeley, CA 94720–7450, USA. ¹³Expense Reduction Consulting, Inc., NASA Johnson Space Center, Houston, TX 77058, USA. ¹⁴Geophysical Laboratory, Carnegie Institution of Washington, Washington, DC 20015, USA. ¹⁵Exobiology Branch, NASA-Ames Research Center, Moffett Field, CA 94035, USA. ¹⁶Goddard Center for Astrobiology, NASA-Goddard Space Flight Center, Greenbelt, MD 20771, USA. ¹⁷Novatech s.r.l., Città della Scienza, via Cordoglio 57d, 80124 Napoli, Italy. ¹⁸Physics and Astronomy Department, State University of New York at Stony Brook, Stony Brook, NY 11794–3800, USA. ¹⁹Department of Physics, State University of New York at Plattsburgh, Plattsburgh, NY 12901, USA. ²⁰Planetary and Space Sciences Research Institute, Open University, Milton Keynes, MK7 6AA, UK. ²¹Chemical Science Division, Lawrence Berkeley National Laboratory, Berkeley, CA 94720–8225, USA. ²²Laboratoire d'Etude de la Matière Extraterrestre, Muséum National d'Histoire Naturelle, Paris, France. ²³NASA, Johnson Space Center, Houston, TX 77058, USA. ²⁴Advanced Light Source, Lawrence Berkeley National Laboratory, Berkeley, CA 94720–8225, USA. ²⁵Institut für Planetologie, Westfälische Wilhelms-Universität Münster, Wilhelm-Klemm-Strasse 10, 48149 Münster, Germany. ²⁶Science Division, Jet Propulsion Laboratory, 4800 Oak Grove Drive, Pasadena, CA 91109, USA. ²⁷Dipartimento Scienze Applicate, Università degli Studi di Napoli “Parthenope,” Napoli 80133, Italy. ²⁸Department of Chemistry, Stanford University, Stanford, CA 94305–5080, USA. ²⁹Department of Physics and McDonnell Center for the Space Sciences, Washington University, St. Louis, MO 63130, USA. ³⁰Department of Earth and Planetary Sciences and McDonnell Center for the Space Sciences, Washington University, St. Louis, MO 63130–4899, USA. ³¹Astromaterials Research and Exploration Science, NASA, Johnson Space Center, Houston, TX 77058, USA.

*To whom correspondence should be addressed. E-mail: ssandford@mail.arc.nasa.gov

meteorites and IDPs (fig. S2A). For example, track 16 has a surface covered relatively uniformly with aromatic molecules. The organic mass distribution in this track was intermediate between typical spectra from primitive chondrites and individual IDPs. In the 78 to 300 atomic mass unit (amu) range, the predominant observed species are naphthalene ($C_{10}H_8$) (2 rings, 128 amu), phenanthrene ($C_{14}H_{10}$) (3 rings, 178 amu), and pyrene ($C_{16}H_{10}$) (4 rings, 202 amu), along with their alkylated homologs extending up to at least C_4 -alkyl. This distribution strongly resembles that of matrix material in the Murchison carbonaceous chondrite and some IDPs (7). However, additional peaks not accounted for by simple 2-, 3-, and 4-ring C_n -alkyl-aromatics imply a more diverse suite of organics than found in Murchison. Peaks at 101, 112, 155, and 167 amu, inconsistent with simple PAHs, were observed when an attenuated laser photoionization pulse was used to minimize photo-fragmentation. These peaks could be due to O- and N-substituted aromatic species having hetero-functionality external to the aromatic structure, that is, not N- or O-heterocyclics. Similar mass peaks have been observed in several IDPs (7). The similarity to IDPs extends to masses beyond 300 amu; several track spectra show mass envelopes extending up to 800 amu with both odd and even mass peaks (fig. S2B). Such high-mass envelopes in IDPs have been attributed to polymerization of smaller aromatics within the samples by radiation processing during their extended exposure to interplanetary space or heating during atmospheric entry. Modification of the original

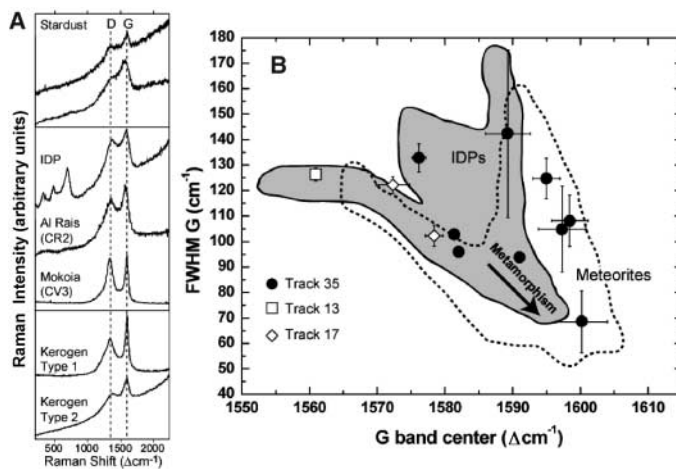
PAH population by heating may also explain the higher mass envelopes observed in these Stardust impact tracks.

PAHs were also seen by TOF-SIMS analyses of a terminal particle extracted from aerogel (track 44, grain 4), a dissected aerogel keystone with a particle track split down the middle (track 21), and residues found in a large crater on Al foil C2009N. All PAHs were correlated to the presence of grains or the impact feature (fig. S3, B and C). Cometary samples from track and terminal particles typically show a steep decrease in PAH abundances with increasing number of C atoms in TOF-SIMS data, but this dependence is weaker for the crater residue (fig. S3A). This fractionation may be due to preferential loss of smaller PAHs during impact on the foil compared with the less violent deceleration into aerogel.

Aromatic materials are also seen using Raman spectroscopy. Raman spectra, acquired for 12 Stardust particles extracted from tracks 13 (1 particle), 17 (2 particles), and 35 (9 particles), are dominated by two broad bands centered at $\sim 1360 \Delta\text{cm}^{-1}$ and $\sim 1580 \Delta\text{cm}^{-1}$ (Fig. 1). These “D” and “G” bands, respectively, are characteristic of “disordered carbonaceous material”—graphite-like sp^2 -bonded carbon in the form of condensed carbon rings. Relative peak sizes, peak positions, and widths of the D and G bands reflect the degree of disorder of the material and can provide constraints on the degree of thermal metamorphism experienced by organic materials (8, 9).

The Raman spectra of the 12 Stardust particles are qualitatively similar to those of many IDPs and

Fig. 1. (A) Raman spectra of Stardust particles from track 35, grain 30 and track 13, grain 1 (top pair) compared with the spectra of organics from extraterrestrial (middle three) and terrestrial (bottom pair) carbonaceous materials with different fluorescence backgrounds. All exhibit D and G bands characteristic of disordered sp^2 -bonded carbon. The phyllosilicate bands below 1000 cm^{-1} in the IDP spectrum have not been seen in Stardust samples. **(B)** The G band position and width [full width at half maximum (FWHM)] of a material reflect its degree of thermal metamorphism and “structural ordering.” The boundaries show the range of values from more than 40 chondritic meteorites (unshaded area with dashed outline) and 40 IDPs (shaded area with solid outline) analyzed in PET Raman laboratories (9, 10, 29). Analyzed Stardust particles (points) span the entire range seen in IDPs and meteorites. Organics in highly thermally metamorphosed meteorites plot to the lower right. The presence of Stardust points in the upper left indicates that at least some of the cometary organics are very primitive and were captured with relatively little alteration. One Stardust sample shows an unusually low G-band position (below 1570 cm^{-1}), suggesting diamond-like carbon that has been amorphized, for example, due to particle irradiation (30). One-sigma error bars represent measurement reproducibility and do not include estimates of possible interlaboratory biases.



of a material reflect its degree of thermal metamorphism and “structural ordering.” The boundaries show the range of values from more than 40 chondritic meteorites (unshaded area with dashed outline) and 40 IDPs (shaded area with solid outline) analyzed in PET Raman laboratories (9, 10, 29). Analyzed Stardust particles (points) span the entire range seen in IDPs and meteorites. Organics in highly thermally metamorphosed meteorites plot to the lower right. The presence of Stardust points in the upper left indicates that at least some of the cometary organics are very primitive and were captured with relatively little alteration. One Stardust sample shows an unusually low G-band position (below 1570 cm^{-1}), suggesting diamond-like carbon that has been amorphized, for example, due to particle irradiation (30). One-sigma error bars represent measurement reproducibility and do not include estimates of possible interlaboratory biases.

primitive meteorites (Fig. 1 and fig. S4), indicating the presence of relatively unmetamorphosed organic matter. The G-band parameters of the Stardust samples span the range observed in IDPs and meteorites (Fig. 1B). It is not clear whether this variation reflects heterogeneity in the cometary samples or variable processing during aerogel impact. However, the presence of points in the upper left of the plot indicates that at least some organics were captured with relatively little alteration. A variety of carbonaceous materials exhibit the D and G bands, including disordered graphite, large PAHs, and “kerogens” (aromatic moieties linked together in a disordered manner). These materials contain condensed aromatic rings but differ in chemical composition. In addition to C and H, meteoritic macromolecular organics contain substantial amounts of O, N, and S, both in the aromatic rings and in cross-linked side chains. Raman spectra can reflect such compositional differences in the overall fluorescent background of the spectrum. Many Raman spectra of Stardust particles are characterized by very high and increasing backgrounds similar to the spectra obtained from type II kerogen, some deuterium-rich IDPs (10), and primitive meteorites, indicating that the samples may be rich in noncarbon heteroatoms such as N, as confirmed by XANES and SIMS results [see below and (11)]. In a few cases, aromatic materials have also been identified by infrared (IR) spectroscopy (6).

IR spectra taken from tracks and individual extracted particles provide evidence for the presence of other, nonaromatic chemical functional groups. IR spectra of particles and tracks often contain absorption features at 3322 cm^{-1} (–OH), 3065 cm^{-1} (aromatic CH), 2968 cm^{-1} (–CH₃), 2923 cm^{-1} (–CH₂–), 2855 cm^{-1} (–CH₃ and –CH₂–), and 1706 cm^{-1} (C=O) (Fig. 2 and figs. S5 and S6) (12). When present, these features are particularly intense along the track walls. IR reflectance spectra of individual grains removed from impact tracks and pressed into Au substrates exhibit similar absorption features. One particle (track 35, grain 26) also showed a weak 2232 cm^{-1} band possibly due to $\text{C}\equiv\text{N}$ stretching vibrations. Raman spectra of three Stardust samples (track 35, grain 30; track 35, grain 32; and track 41, grain 7) are also consistent with the presence of alkane-type saturated hydrocarbons (fig. S4). Combined, these spectra data indicate the presence of aromatic, aliphatic, carboxylic, and N-containing functional groups.

The observed $\text{–CH}_2\text{–}$ (2923 cm^{-1})/ –CH_3 (2968 cm^{-1}) band-depth ratios in the returned samples is typically ~ 2.5 (12). This band-depth ratio is similar to the average value from IR spectra of anhydrous IDPs (13) but considerably larger than that seen in macromolecular material in primitive carbonaceous chondrites (~ 1.1) and the diffuse interstellar medium (ISM) (1.1 to 1.25). This suggests that the aliphatic moieties in Wild-2 particles are longer or less branched than those in the diffuse ISM. The

Stardust

band depth ratio of ~ 2.5 corresponds to a functional group ratio of $-\text{CH}_2-/-\text{CH}_3 \sim 3.7$ in the Wild 2 samples, assuming typical intrinsic band strengths for these features (14). The ratio of aromatic to aliphatic C-H is quite variable, with C-H stretching aromatic/aliphatic optical depth

ratios ranging from below the detection limit to ~ 0.1 (6).

C,N,O-XANES analyses of thin sections of individual grains confirm the presence of $1s-\pi^*$ transitions consistent with variable abundances of aromatic, keto/aldehydic, and carboxyl moieties,

Fig. 2. IR transmittance spectra obtained along a line perpendicular to cometary impact tracks (A) track 59 and (B) track 61. In addition to aerogel features, the spectra of track 59 (A) display peaks at 3322 (broad), 2968, 2923, 2855, and 1706 cm^{-1} (not shown), both inside the track and extending outward into the aerogel. (B) track 61 exhibits only the aliphatic CH stretching feature dominated by the 2968 cm^{-1} peak and (Si-O) bands (not shown) characteristic of the flight aerogel. The optical images of the same tracks, with corresponding maps to the same scale showing the intensity distribution of the 2923 cm^{-1} peak ($-\text{CH}_2-$), are displayed in (C) and (D). The false-color image scale shown at the bottom is used in both maps, and the black scale bars correspond to 100 μm . In both cases, the entrance of the cometary particle is on the left side. The false-color map in (C) shows an increase in intensity of the 2923 cm^{-1} $-\text{CH}_2-$ peak in and near the track. The distributions of other organics peaks are similar. In contrast, the second track shown in (D) shows almost uniform distribution of the peak area centered at 2923 cm^{-1} ; that is, the track shows only the features of aerogel.

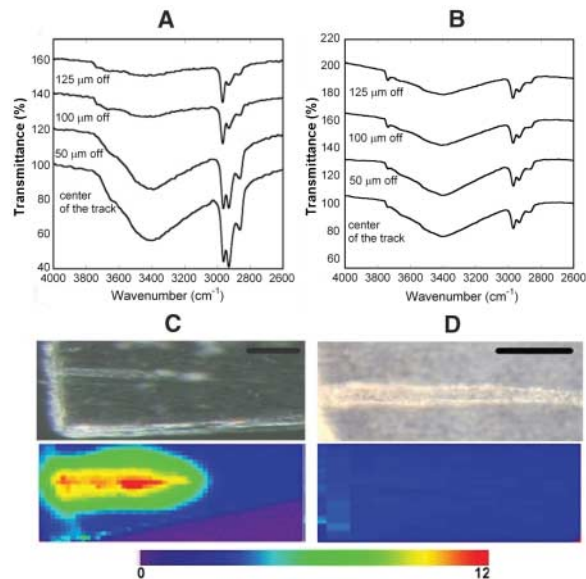
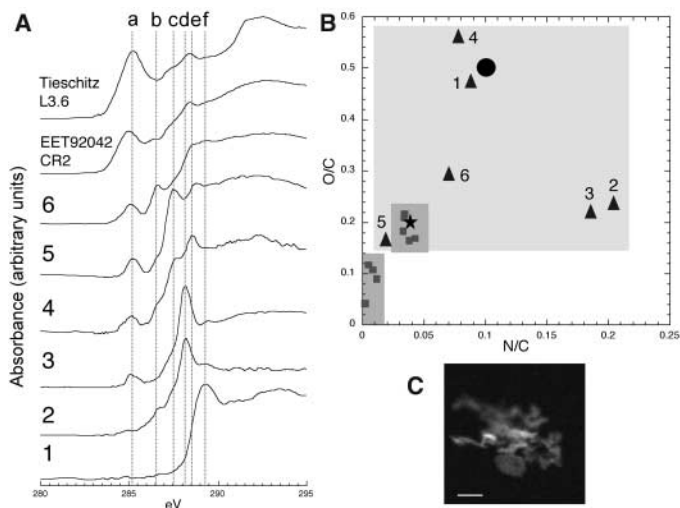


Fig. 3. (A) C-XANES spectra of six thin-section samples (1 to 6) compared with spectra of primitive (EET92042, CR2) and moderately processed (Tieschitz, L3.6) chondritic organic matter. Samples are 1, track 16, grain 1, mount 10; 2, track 35, grain 16, mount 4; 3, track 22, grain 1, mount 5; 4, track 35, grain 32, mount 10; 5, track 35, grain 32, mount 8; and 6, (track 13, grain, mount 5) (samples 4 and 5 are different thin sections of the same grain). Specific organic functional groups are highlighted (dashed lines a to f). a, C=C at ~ 285.2 eV; b, C=C-O at ~ 286.5 eV; c, C=O at ~ 287.5 eV; d, N=C=O at 288.2 eV; e, O=C=O at 288.6 eV; and f, C-O at 289.5 eV. Sample chemistry ranges enormously, with sp^2 -bonded carbon varying from nonexistent in sample 1 to modest in samples 5 and 6 (relative to chondritic organic matter). (B) Atomic O/C and N/C for samples 1 to 6 derived from C,N,O-XANES analysis (black triangles) are compared with chondritic organic matter (gray squares, where the higher values correspond to petrologic type 1 and 2 and the lower values are type 3). Average values for comet Halley particles and stratospheric IDPs (15, 16) are marked by a black star and a large solid circle, respectively. (C) An example of a sample thin section from track 35, grain 32, mount 8 (spectrum 5) revealed as a high-resolution (40-nm pixel size) STXM optical density image (scale bar, 1 μm) on the carbon 1s absorption edge.



as well as amides and nitriles (Fig. 3A). XANES data suggest that considerably less H- and C-substituted sp^2 -bonded C (olefinic and aromatic) is present than in highly primitive chondritic organic matter. Aliphatic C likely contributes to spectral intensity around 288 eV in most of the particles. One particle (particle 1 in Fig. 3A) has remarkably simple C chemistry, consistent with a predominance of alcohol and/or ether moieties. However, the XANES data generally indicate complex molecular structures variably rich in heteroatoms O and N and, compared with the macromolecular material in primitive meteorites, containing additional materials that are relatively poor in aromatic and olefinic C. The high abundances of heteroatoms and the low concentration of aromatic C in these organics differ greatly from the acid insoluble organic matter in meteorites and, in terms of thermal processing, appear to be more primitive.

XANES provides quantitative estimates of atomic O/C and N/C ratios present in the various functional groups identified (6). Care must be taken to account for O from any associated silicates or aerogel. Figure 3B shows that five of six organic-rich particles are richer in the heteroatoms O and N relative to both chondritic organic matter and the average composition of comet P/Halley particles measured by Giotto (15). The values are, however, qualitatively similar to the average O/C and N/C reported for stratospheric IDPs (16). Particles with such high O/C and N/C ratios are likely to be relatively labile [see below and (6)].

Particles 2 and 3 are particularly rich in N and exhibit abundant amide C in their XANES spectra (Fig. 3A). The presence of N-containing compounds is further suggested by studies of collector aerogel using LC-FD/TOF-MS. Although PET attention has largely focused on impacts in the aerogel and Al foils, Stardust may have returned a “diffuse” sample of gas-phase molecules that struck the aerogel directly or that diffused away from grains after impact. To test this possibility, samples of flight aerogel were carried through a hot water extraction and acid hydrolysis procedure (17) to determine if primary amine compounds were present in excess of those seen in controls.

With the exception of methylamine (MA) and ethylamine (EA), all amines detected in Stardust aerogel samples cell 2054, aerogel fragment 4 (hereafter C2054,4) and cell 2086, aerogel fragment 1 (hereafter C2088,1) were also present in the witness coupon aerogel sample (WCARM11CPN,9). The absolute abundances of MA and EA are much higher, and the molar ratio of MA to EA in Stardust comet-exposed aerogel (C2054,4: 1.0 ± 0.1 ; C2086,1: 1.8 ± 0.2) is distinct from preflight aerogel (flight spare aerogel cell E243-13C, unflown: 10 ± 3) (6). The absence of MA and EA in the aerogel witness coupon suggests that these amines are cometary in origin. The concentrations of MA and EA in C2054,4 (0.6 to 2.2 parts per million) were similar to those present in C086,1, which was not located adjacent to a par-

track, suggesting that these amines, if cometary, originate from submicron particles or gas that directly impacted the collector. Glycine is also present in samples C2054,4 and C086,1 at relative abundances that exceed those found in controls. This may indicate that a cometary component for this amino acid is also present. Compound-specific isotope measurements will be necessary to constrain the origin of these amines. No MA, EA, or glycine was detected in non-acid-hydrolyzed aerogel extracts. This suggests that these amines are present in an acid-soluble bound form rather than as a free primary amine. These results are consistent with the XANES detection of an amine-rich organic polymer in some of the recovered particles.

Raman (Fig. 1B), XANES (Fig. 3), and isotopic (*II*) data all demonstrate that the distribution of organics (overall abundance, functionality, and relative elemental abundances of C, N, and O) is heterogeneous both within particles and between particles. The STXM XANES results show variations in the physical distribution of these materials within particles, and the IR mapping of particle tracks (Fig. 2) shows the presence of organic features in some impact tracks but not others. The degree to which these variations represent heterogeneity in the original samples versus differences in impact processing is currently not fully constrained. On the whole, the chemical variations suggest that cometary organics do not represent an equilibrated reservoir of materials.

Most of the organic material in meteorites is in insoluble macromolecular phases. In contrast, the Stardust samples show evidence of abundant, relatively labile organics. In many cases, the or-

ganic components that produce the $-OH$, $-CH_3$, $-CH_2-$, and $C=O$ IR absorption bands extend well beyond the visible edge of the track (Fig. 2). This suggests that the incoming particles contained organics that volatilized during impact and diffused into the surrounding aerogel. This material is unlikely to be due to impact-altered C from the aerogel because similar tracks are seen in the same aerogels that show no IR-detectable organics beyond those seen in the original aerogel (Fig. 2). All impacting particles had identical velocities, and tracks of similar length probably had similar impact energies. Consequently, similar amounts of organics would be expected in all tracks if this material came solely from reprocessing of C in the aerogel. Also, if impact-driven oxidation of C in the aerogel was occurring, the $C=O$ band might be expected to be seen in and around all tracks, but this feature is only seen in tracks with the other organic features. Finally, locations near tracks show no deficits of the $-CH_3$ original to the aerogel, implying that the original C has not been substantially converted to other forms.

Hydrogen isotopic measurements were made by SIMS in fragments of five particles (*II*). D/H enrichments up to three times terrestrial were observed in three of five measured samples. D enrichments are often seen in meteoritic and IDP organics and are thought to be due to materials with an interstellar/protostellar chemical heritage (18–20). In all cases, the D-rich H is heterogeneously distributed within the samples and is associated with C, indicating it is organic. The elevated D/H ratios are comparable to those of many IDPs and meteoritic samples, although none of the cometary samples examined to date have

shown ratios as extreme as the most anomalous values measured in some IDPs, meteorites, and some cometary coma gases.

Isotopic anomalies are also observed in C and N (*II*). As with IDPs and meteorites, these anomalies often appear in the form of “hot spots” that differ from the surrounding particle. NanoSIMS ion imaging demonstrates that N and S are associated with organic molecules (Fig. 4). The samples show a distribution of N/C ratios ranging from 0.005 to values approaching 1. Some particles exhibit the entire range of values, whereas others fall more uniformly at the high N/C end of the range, consistent with the XANES data (Fig. 3B). However, there are regions with high C content that are not rich in N. Sulfur is typically associated with C and N but is also distributed in small hot spots, presumably due to sulfides, which are commonly seen in the returned samples (21).

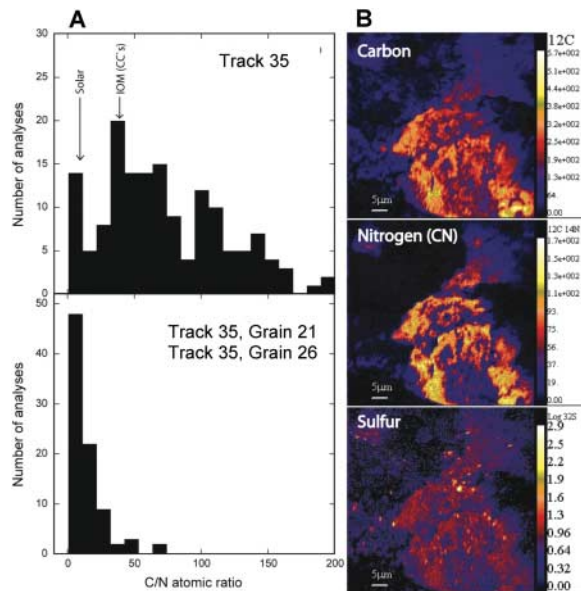
When observed, the D and/or ^{15}N enhancements provide clear evidence of a cometary origin for the organics and suggest that cometary organics contain a population with an interstellar/protostellar chemical heritage. Particles with measured isotopic anomalies are represented among the samples studied by other techniques by the Organics PET. For example, FC9,0,13,1,0 (track 13, grain 1) (particle 6 in Fig. 3) was examined by XANES, and track 13, particle 1; track 17, grain 1; and track 35, grain 25 were measured by Raman.

In terms of sample heterogeneity, the organics found in Stardust samples are similar to stratospheric IDPs and primitive meteorites. Like meteoritic organic matter, they contain both aromatic and nonaromatic fractions. However, the Stardust samples exhibit a greater range of compositions (higher O and N concentrations), include an abundant organic component that is poor in aromatics, and contain a more labile fraction. These latter two “components” could possibly be accounted for by a single population of organics. The nonaromatic fraction appears to be far more abundant, relative to aromatics, than is seen in meteorites. In general terms, the organics in Stardust samples are even more “primitive” than those in meteorites and IDPs, at least in terms of being highly heterogeneous and unequilibrated.

The Cometary and Interstellar Dust Analyzer (CIDA) TOF-MS instrument on the Stardust spacecraft detected very few particle impacts during the flyby (22). However, some of the returned mass spectra suggest the presence of particles with a nitrogen-rich chemistry and lower abundances of O, implying that nitriles or polycyanides may have been present (22). Although direct comparisons are not possible, studies of the samples confirm that N-rich components are present in the dust.

The presence of high O and N contents and the high ratios of $-CH_2-$ / $-CH_3$ seen in the infrared data indicate that the Stardust organics are not similar to the organic materials seen in the diffuse ISM, which look more similar to the insoluble macromolecular material seen in primitive mete-

Fig. 4. Distribution of C and N. **(A)** Histograms of C/N ratios in organics in three different Stardust samples. One sample (top) shows a large spread in C/N, whereas two samples (bottom) have organics characterized by low C/N ratios, consistent with the presence of volatile organic molecules such as HCN or their polymer counterparts. **(B)** NanoSIMS images of the distribution of C, N, and S in a region of an aerogel sample from along track 35 containing cometary materials. The intensity of the signal increases from blue to red to bright yellow. C, N, and S distributions are clearly correlated, although considerable variations in their relative abundances are observed. S is also present in a population of hot spots that likely indicate the presence of sulfides.



The color scale in the S map is logarithmic, in order to show the large difference in S count rates between the organics and the sulfides. The distribution of C and N is qualitatively similar in particles both with and without ^{15}N excesses. The location labeled IOM (CCs) in the upper left panel denotes the C/N ratio of the insoluble organic matter found in carbonaceous chondrites.

rites, but with even lower O/C ratios (23). This suggests that the Stardust organics are not the direct result of stellar ejecta or diffuse ISM processes but rather result from dense cloud and/or protosolar nebular processes. The high O and N contents, lower aromatic contents, and elevated $-\text{CH}_2-/-\text{CH}_3$ ratios are all qualitatively consistent with what is expected from radiation processing of astrophysical ices and the polymerization of simple species such as HCO, H_2CO , and HCN (24–26).

The Stardust samples clearly contain an organic component that is more labile than the materials seen in meteorites and IDPs. These labile materials may be absent from stratospheric IDPs because they are lost during atmospheric entry heating and/or are destroyed or modified by radiation during the IDPs' transit from parent body to Earth. Given the O- and N-rich nature of the Stardust materials, these labile organics could represent a class of materials that have been suggested as parent molecules to explain the extended coma sources of some molecular fragments like CN (27, 28). The high O/C and N/C ratios of the samples fall well outside the range of most meteorites and, interestingly enough, reach higher values than those observed at comet Halley by the Giotto spacecraft (15). In this respect, some of the returned material appears to

represent a new class of organics not previously observed in other extraterrestrial samples.

References and Notes

1. M. C. Festou, H. U. Keller, H. A. Weaver, Eds., *Comets II* (Univ. of Arizona Press, Tucson, AZ, 2004).
2. A. H. Delsemme, *Adv. Space Res.* **12**, 5 (1992).
3. C. F. Chyba, C. Sagan, *Nature* **355**, 125 (1992).
4. D. E. Brownlee et al., *J. Geophys. Res.* **108**, E10, 8111, p. 1–1 (2003).
5. D. E. Brownlee et al., *Science* **314**, 1711 (2006).
6. Materials and methods are available as supporting material on Science Online.
7. S. Clemett, C. Maechling, R. Zare, P. Swan, R. Walker, *Science* **262**, 721 (1993).
8. B. Wopenka, J. D. Pasteris, *Am. Mineral.* **78**, 533 (1993).
9. L. Bonal, E. Quirico, M. Bourot-Denise, G. Montagnac, *Geochim. Cosmochim. Acta* **70**, 1849 (2006).
10. B. Wopenka, *EPSL* **88**, 221 (1988).
11. K. D. McKeegan et al., *Science* **314**, 1724 (2006).
12. L. P. Keller et al., *Science* **314**, 1728 (2006).
13. G. Matrajt et al., *Astron. Astrophys.* **433**, 979 (2005).
14. S. A. Sandford et al., *Astrophys. J.* **371**, 607 (1991).
15. J. Kissel, F. R. Krueger, *Nature* **326**, 755 (1987).
16. G. J. Flynn, L. P. Keller, S. Wirick, C. Jacobsen, *Proceedings of the 8th International Conference on X-ray Microscopy*, IPAP Conf. Series **7**, 315 (2006).
17. D. P. Glavin et al., *Meteorit. Planet. Sci.* **41**, 889 (2006).
18. S. Messenger, *Nature* **404**, 968 (2000).
19. J. Aléon, F. Robert, *Icarus* **167**, 424 (2004).
20. H. Busemann et al., *Science* **312**, 727 (2006).
21. M. E. Zolensky et al., *Science* **314**, 1741 (2006).

22. J. Kissel, F. R. Krueger, J. Silén, B. C. Clark, *Science* **304**, 1774 (2004).
23. Y. J. Pendleton, L. J. Allamandola, *Astrophys. J. Suppl. Ser.* **138**, 75 (2002).
24. M. P. Bernstein, S. A. Sandford, L. J. Allamandola, S. Chang, M. A. Scharberg, *Astrophys. J.* **454**, 327 (1995).
25. W. A. Schutte, L. J. Allamandola, S. A. Sandford, *Icarus* **104**, 118 (1993).
26. G. Strazzulla, G. A. Baratta, M. E. Palumbo, *Spectrochim. Acta A* **57**, 825 (2001).
27. M. J. Mumma, P. R. Weissman, S. A. Stern, in *Protostars and Planets III*, E. H. Levy, J. I. Lunine, M. S. Matthews, Eds. (Univ. of Arizona Press, Tucson, AZ, 1993), pp. 1171–1252.
28. G. Strazzulla, *Space Sci. Rev.* **90**, 269 (1999).
29. E. Quirico, J. Borg, P.-I. Raynal, G. Montagnac, L. D'Hendecourt, *Planet. Space Sci.* **53**, 1443 (2005).
30. G. A. Baratta et al., *J. Raman Spectrosc.* **35**, 487 (2004).
31. The Stardust Organics Preliminary Examination Team is grateful to NASA for funding and supporting the mission and to the hundreds of other team members that were involved in design, construction, flying, and recovery of the mission. The Organics Team, from 31 organizations, gratefully acknowledges their supporting institutions.

Supporting Online Material

www.sciencemag.org/cgi/content/full/314/5806/1720/DC1
Materials and Methods
Figs. S1 to S9
References

3 October 2006; accepted 9 November 2006
10.1126/science.1135841

REPORT

Isotopic Compositions of Cometary Matter Returned by Stardust

Kevin D. McKeegan,^{1*} Jerome Aléon,^{2,3,4} John Bradley,³ Donald Brownlee,⁵ Henner Busemann,⁶ Anna Butterworth,⁷ Marc Chaussidon,⁸ Stewart Fallon,^{3,4} Christine Floss,⁹ Jamie Gilmour,¹⁰ Matthieu Gounelle,¹¹ Giles Graham,³ Yunbin Guan,¹² Philipp R. Heck,¹³ Peter Hoppe,¹³ Ian D. Hutcheon,^{3,4} Joachim Huth,¹³ Hope Ishii,³ Motoo Ito,¹⁴ Stein B. Jacobsen,¹⁵ Anton Kearsley,¹⁶ Laurie A. Leshin,¹⁷ Ming-Chang Liu,¹ Ian Lyon,¹⁰ Kuljeet Marhas,⁹ Bernard Marty,⁸ Graciela Matrajt,⁵ Anders Meibom,¹¹ Scott Messenger,¹⁴ Smail Mostefaoui,¹¹ Sujoy Mukhopadhyay,¹⁵ Keiko Nakamura-Messenger,^{14,18} Larry Nittler,⁶ Russ Palma,^{19,20} Robert O. Pepin,²⁰ Dimitri A. Papanastassiou,²¹ François Robert,¹¹ Dennis Schlutter,²⁰ Christopher J. Snead,⁷ Frank J. Stadermann,⁹ Rhonda Stroud,²² Peter Tsou,²¹ Andrew Westphal,⁷ Edward D. Young,¹ Karen Ziegler,¹ Laurent Zimmermann,⁸ Ernst Zinner⁹

Hydrogen, carbon, nitrogen, and oxygen isotopic compositions are heterogeneous among comet 81P/Wild 2 particle fragments; however, extreme isotopic anomalies are rare, indicating that the comet is not a pristine aggregate of presolar materials. Nonterrestrial nitrogen and neon isotope ratios suggest that indigenous organic matter and highly volatile materials were successfully collected. Except for a single ^{17}O -enriched circumstellar stardust grain, silicate and oxide minerals have oxygen isotopic compositions consistent with solar system origin. One refractory grain is ^{16}O -enriched, like refractory inclusions in meteorites, suggesting that Wild 2 contains material formed at high temperature in the inner solar system and transported to the Kuiper belt before comet accretion.

The isotopic compositions of primitive solar system materials record evidence of chemical and physical processes involved in the formation of planetary bodies ~4.6 billion years ago and, in some cases, provide a link to materials and processes in the molecular cloud that predated our solar system. The vast majority of

isotopic analyses of extraterrestrial materials have been performed on chondritic (undifferentiated) meteorites, samples of asteroids that likely accreted at 2 to 4 astronomical units (AU) within the first few million years of solar system history. Comets formed in much colder regions of the protoplanetary disk and are widely considered to

consist of more primitive matter than even the most unequilibrated meteorites.

Analyses of isotope compositions of comets are rare. Measurements of D/H, $^{13}\text{C}/^{12}\text{C}$, $^{15}\text{N}/^{14}\text{N}$, or $^{18}\text{O}/^{16}\text{O}$ have been made for a few abundant molecules in gases of several comet comae by ground-based spectroscopy (1–3) and of comet P/Halley by mass spectrometers on the Giotto spacecraft (4). Direct measurements of isotope compositions in the dust fraction of comets are limited to low-precision data from the Halley flyby (5). Isotopic measurements of stratosphere-collected interplanetary dust particles (IDPs) demonstrate the highly primitive nature of many anhydrous IDPs [e.g., (6, 7)]; however, a cometary origin for specific individual particles cannot be ascertained. Here, we report laboratory analyses of the light “stable” isotopes of H, C, N, O, and Ne in individual grains, particle fragments, crater debris, and/or trapped volatile materials collected from comet 81P/Wild 2 and returned to Earth by the NASA Discovery Mission, Stardust.

The goals of the Isotope Preliminary Examination Team analyses are to provide first-order answers to questions relating to the provenance of Wild 2 dust: (i) Does the comet consist of a mechanical agglomeration of essentially unprocessed, or perhaps only thermally annealed, presolar materials? (ii) Do comets provide a well-preserved reservoir of circumstellar dust grains (8) with distinct nucleosynthetic histories (i.e., stardust)? (iii) Can isotopic signatures establish whether extraterrestrial organic materials are present above contamination levels? (iv) What are the

Organics Captured from Comet 81P/Wild 2 by the Stardust Spacecraft

Scott A. Sandford, Jérôme Aléon, Conel M. O'D. Alexander, Tohru Araki, Sas?a Bajt, Giuseppe A. Baratta, Janet Borg, John P. Bradley, Donald E. Brownlee, John R. Brucato, Mark J. Burchell, Henner Busemann, Anna Butterworth, Simon J. Clemett, George Cody, Luigi Colangeli, George Cooper, Louis D'Hendecourt, Zahia Djouadi, Jason P. Dworkin, Gianluca Ferrini, Holger Fleckenstein, George J. Flynn, Ian A. Franchi, Marc Fries, Mary K. Gilles, Daniel P. Glavin, Matthieu Gounelle, Faustine Grossemy, Chris Jacobsen, Lindsay P. Keller, A. L. David Kilcoyne, Jan Leitner, Graciela Matrajt, Anders Meibom, Vito Mennella, Smail Mostefaoui, Larry R. Nittler, Maria E. Palumbo, Dimitri A. Papanastassiou, François Robert, Alessandra Rotundi, Christopher J. Snead, Maegan K. Spencer, Frank J. Stadermann, Andrew Steele, Thomas Stephan, Peter Tsou, Tolek Tylliszczak, Andrew J. Westphal, Sue Wirick, Brigitte Wopenka, Hikaru Yabuta, Richard N. Zare and Michael E. Zolensky

Science **314** (5806), 1720-1724.
DOI: 10.1126/science.1135841

ARTICLE TOOLS

<http://science.sciencemag.org/content/314/5806/1720>

SUPPLEMENTARY MATERIALS

<http://science.sciencemag.org/content/suppl/2006/12/11/314.5806.1720.DC1>

RELATED CONTENT

<http://science.sciencemag.org/content/sci/314/5806/1708.full>
<http://science.sciencemag.org/content/sci/314/5806/1711.full>
<http://science.sciencemag.org/content/sci/314/5806/1707.full>
<http://science.sciencemag.org/content/sci/317/5845/1680.3.full>
<http://science.sciencemag.org/content/sci/317/5845/1680.2.full>
<http://science.sciencemag.org/content/sci/314/5806/1728.full>
<http://science.sciencemag.org/content/sci/314/5806/1731.full>
<http://science.sciencemag.org/content/sci/314/5806/1716.full>
<http://science.sciencemag.org/content/sci/314/5806/1735.full>
<http://science.sciencemag.org/content/sci/314/5806/1724.full>
<http://science.sciencemag.org/content/sci/314/5806/1709.full>
file:/contentpending:yes

REFERENCES

This article cites 27 articles, 7 of which you can access for free
<http://science.sciencemag.org/content/314/5806/1720#BIBL>

PERMISSIONS

<http://www.sciencemag.org/help/reprints-and-permissions>

Use of this article is subject to the [Terms of Service](#)

Science (print ISSN 0036-8075; online ISSN 1095-9203) is published by the American Association for the Advancement of Science, 1200 New York Avenue NW, Washington, DC 20005. 2017 © The Authors, some rights reserved; exclusive licensee American Association for the Advancement of Science. No claim to original U.S. Government Works. The title *Science* is a registered trademark of AAAS.